Dehydrogenation of Methane by Gas-Phase Os^+: A Density Functional Study

Ganbing Zhang, Shuhua Li,* and Yuansheng Jiang

Department of Chemistry, Institute of Theoretical and Computational Chemistry, Lab of Mesoscopic Materials Science, Nanjing University, Nanjing, 210093, People's Republic of China

Received April 22, 2003

Density functional calculations have been performed to explore the sextet, quartet, and doublet potential energy surfaces of methane dehydrogenation by gas-phase Os^+ for understanding the reaction mechanism. The minimum energy reaction path is found to involve the spin inversion three times in the different reaction steps. Totally, three spin states (sextet, quartet, and doublet) are involved in the whole reaction. Specifically, the reaction is most likely to proceed through the following steps: $^6Os^+ + CH_4 \rightarrow OsCH_4^+$ (^{6}**1**) $\rightarrow HOsCH_3$ (^{4}**2**) $\rightarrow HOsH(CH_2)^+$ (^{2}**3**) $\rightarrow (H_2)Os(CH_2)^+$ (^{4}**4**) $\rightarrow Os(CH_2)^+$ (^{4}**5**) $+ H_2$. The overall reaction is calculated to be exothermic by 4.2 kcal/mol, which is in good agreement with the available experimental results. The first spin inversion, from the sextet state to the quartet state, makes the activation of the first C−H bond energetically spontaneous. The second transition from the quartet state to the doublet state facilitates the cleavage of the second C−H bond, lowering the barrier from 25.9 kcal/mol to 16.1 kcal/mol. The third spin inversion occurs from the doublet state to the quartet state in the reductive elimination step of H_2, and this spin inversion leads to a decrease in the barrier height from 41.0 to 30.4 kcal/mol.

1. Introduction

During the past decades the C−H and C−C bond activations of small alkanes and olefins in the gas phase by transition-metal ions have received a great deal of attention both experimentally and theoretically for the potential economic and environmental significance and considerable fundamental interest.[1] As the simplest hydride of carbon and the principal constituent of natural gas, inert methane activation by bare transition-metal cations M^+ has especially been at the focus of a number of fundamental gas-phase ion organometallic chemistries.[1d,i,r,2−7] On one hand, the activation of the C−H bond in methane is a unique challenge among the hydrocarbons due to its unusual strength (e.g., the C−H bond energy in methane (105 kcal/mol) is about 5 kcal/mol greater than that in ethane).[7] Thus, the activation of the C−H bond in methane has been the long-term task for chemists.[7−9] On the other hand, the mechanistic details of the activation process of the C−H and C−C bonds in the gas phase can be readily obtained, because many complicated factors such as solvent, ligands, surface, and aggregation effects occurring on surfaces or in solutions are excluded.[1]

Early in 1979 Allison et al. already discovered that atomic transition metal cations are capable of activating C−H bonds.[10] In the following years there were numerous studies of the reactions of atomic transition-metal ions (M^+) with small alkanes in the gas phase experimentally[1−3,11−19a] and theoretically.[4−6,16−30] In general,

* To whom correspondence should be addressed. E-mail: shuhua@netra.nju.edu.cn. Fax: +86-25-3596131.

(1) (a) Allison, J. *Prog. Inorg. Chem.* **1986**, *34*, 627. (b) Squires, R. R. *Chem. Rev.* **1987**, *87*, 623−646. (c) Russell, D. H., Ed. *Gas-Phase Inorganic Chemistry*; Plenum: New York, 1989. (d) Armentrout, P. B.; Beauchamp, J. L. *Acc. Chem. Res.* **1989**, *22*, 315−321. (e) Armentrout, P. B. *Annu. Rev. Phys. Chem.* **1990**, *41*, 313−344. (f) Jennings, K. R., Ed. *Fundamentals of Gas-Phase Ion Chemistry*; Kluwer Academic Publishers: Dordrecht, 1990. (g) Eller, K.; Schwarz, H. *Chem. Rev.* **1991**, *91*, 1121−1177. (h) Armentrout, P. B. *Science* **1991**, *251*, 175−179. (i) Weisshaar, J. C. *Acc. Chem. Res.* **1993**, *26*, 213−219. (j) Eller, K. *Coord. Chem. Rev.* **1993**, *126*, 93−147. (k) Bowers, M. T. *Acc. Chem. Res.* **1994**, *27*, 324−332. (l) Freiser, B. S. *Acc. Chem. Res.* **1994**, *27*, 353−360. (m) Armentrout, P. B. *Acc. Chem. Res.* **1995**, *28*, 430−436. (n) Armentrout, P. B.; Baer, T. *J. Phys. Chem.* **1996**, *100*, 12866−12877. (o) Freiser, B. S., Ed. *Organometallic Ion Chemistry*; Kluwer Academic Publishers: Dordrecht, 1996. (p) Capron, L.; Mestdagh, H.; Rolando, C. *Coord. Chem. Rev.* **1998**, *178−180*, 269−330. (q) Armentrout, P. B. In *Topics in Organometallic Chemistry*; Brown, J. M., Hofmann, P., Ed.; Springer-Verlag: Berlin, 1999; Vol. 4, pp 1−45. (r) Schwarz, H.; Schröder, D. *Pure Appl. Chem.* **2000**, 72, 2319−2332. (s) Fisher, K. J. *Prog. Inorg. Chem.* **2001**, *50*, 343−432. (t) Armentrout, P. B. *Annu. Rev. Phys. Chem.* **2001**, *52*, 423−461.

(2) (a) Irikura, K. K.; Beauchamp, J. L. *J. Am. Chem. Soc.* **1991**, *113*, 2769−2770. (b) Irikura, K. K.; Beauchamp, J. L. *J. Phys. Chem.* **1991**, *95*, 8344−8351.

(3) Schwarz, H. *Angew. Chem., Int. Ed. Engl.* **1991**, *30*, 820−821.

(4) (a) Hendrickx, M.; Ceulemans, M.; Gong, K.; Vanquickenborne, L. *J. Phys. Chem. A* **1997**, *101*, 2465−2470. (b) Yoshizawa, K.; Suzuki, A.; Yamabe, T. *J. Am. Chem. Soc.* **1999**, *121*, 5266−5273. (c) Yoshizawa, K. *J. Organomet. Chem.* **2001**, *635*, 100−109.

(5) Blomberg, M. R. A.; Siegbahn, P. E. M.; Svensson, M. *J. Phys. Chem.* **1994**, *98*, 2062−2071.

(6) (a) Irikura, K. K.; Goddard, W. A. *J. Am. Chem. Soc.* **1994**, *116*, 8733−8740. (b) Heinemann, C.; Hertwig, R. H.; Wesendrup, R.; Koch, W.; Schwarz, H. *J. Am. Chem. Soc.* **1995**, *117*, 495−500.

(7) (a) Crabtree, R. H. *Chem. Rev.* **1985**, *85*, 245−269. (b) Crabtree, R. H. *Chem. Rev.* **1995**, *95*, 987−1007.

(8) Saillard, J. Y.;Hoffmann, R. *J. Am. Chem.* Soc. **1984,** *106*, 2006−2026.

(9) (a) Rostrup-Nielsen, J. R. *Catal. Today* **2000**, *63*, 159−164. (b) Lunsford, J. H. *Catal. Today* **2000**, *63*, 165−174.

(10) Allison, J.; Freas, R. B.; Ridge, D. P. *J. Am. Chem.* Soc. **1979**, *101*, 1332−1333.

(11) (a) Buckner, S. W.; McMahon, T. J.; Byrd, G. D.; Freiser, B. S. *Inorg. Chem.* **1989**, *28*, 3511−3518. (b) Ranasinghe, Y. A.; MacMahon, T. J.; Freiser, B. S. *J. Phys. Chem.* **1991**, *95*, 7721−7726.

(12) Irikura, K. K.; Beauchamp, J. L. *J. Am. Chem. Soc.* **1989**, *111*, 75−85.

(13) Sunderlin, L. S.; Armentrout, P. B. *J. Am. Chem.* Soc. **1989**, *111*, 3845−3855.

10.1021/om030291v CCC: $25.00
Publication on Web 08/16/2003

alkane dehydrogenation is a common reaction in the gas-phase chemistry of bare transition-metal ions.[1c,2a] However, methane dehydrogenation is very unusual because it is observed at high energies and the excited electronic states of the metal ions are usually involved. Reactions of all first- and second-row M^+ with methane are endothermic,[1d] with the possible exception of Zr^+, which is the only one in the second-row that has been so far found to react with methane exothermically.[11b] The third-row M^+ (M = Ta, W, Os, Ir, and Pt) will spontaneously dehydrogenate methane to form the cationic carbene complexes MCH_2^+ at room temperature[2,11−12] due to their metal−methylene bond strength $D°(M^+-CH_2) \geq 111$ kcal/mol.

Up to now, many theoretical investigations on the mechanism of the reaction of M^+ with CH_4 and the reverse reaction have been performed using different levels of theory, and the detailed potential energy surfaces (PESs) have been obtained for Sc^+,[20] Ti^+,[18b,21] V^+,[21] Cr^+,[21] Fe^+,[22a−c] Co^+,[19a,23,26−27] Rh^+,[25−27] Y^+−Pd^+ (only for the initial C−H-insertion step of the reaction),[5] Ta^+,[28] Ir^+,[27,29] and Pt^+.[16,30] To our knowledge, the detailed potential energy surface for the dehydrogenation of methane by naked Os^+ has not been reported.

Of most interest to the reactions of methane and transition-metal ions is the potential energy surface crossing.[31a] In other words, these reactions may involve a change in the spin states and thus occur in a nonadiabatic way on two or more potential energy surfaces.[31b] Shaik et al. have proposed the two-state reactivity (TSR) should be involved in reactions catalyzed by organometallic systems, in contrast to common organic reactions.[32] A number of reactions in organic, inorganic, and especially organometallic chemistry in which two states of different multiplicities are involved on the reaction pathway have been confirmed by experimental and computational studies.[33−36]

To gain systematic insight into the mechanism of the reaction of third-row transition-metal ions with methane, we present here a theoretical study on the reaction

$$Os^+ + CH_4 \rightarrow OsCH_2^+ + H_2 \qquad (1)$$

To our knowledge, the only experimental report on this reaction was given by Irikura and Beauchamp,[2b,12] who investigated this reaction using Fourier transform ion cyclotron resonance (FTICR) mass spectrometry. Since the reaction was observed under thermochemical conditions, it has to be exothermic or nearly thermoneutral. Besides this, there are few experimental data available for thermochemistry of the studied reaction.

The density functional method, specifically the hybrid functional B3LYP,[37a] is used to investigate the detailed potential energy surfaces of the title reaction in various spin multiplicities since it is proven to be a reliable tool for describing complicated electronic structures in open-shell transition-metal chemistry. To better understand the spin inversion processes involved in the reaction, we determine the energies and structures of the crossing points between two PESs of different spin multiplicities in the reaction pathway. The effect of these crossing points on the energy barriers of different reaction steps is analyzed. We hope the results would deepen our understanding of the mechanism of methane dehydrogenation by gas-phase Os^+.

2. Computational Details

Full optimization of geometries for all stationary points involved in methane dehydrogenation by Os^+ has been calculated using the spin-unrestricted density functional theory (UDFT) method based on the hybrid of Becke's three-parameter exchange functional[37b,c] and the Lee, Yang, and Parr correlation functional[37d] (B3LYP[37a]). In all calculations, for osmium a relativistic effective core potential (RECP)[38] is

(14) Mourgues, P.; Ferhati, A.; McMahon, T. B.; Ohanessian, G. *Organometallics* **1997**, *16*, 210−224.
(15) Wesendrup, R.; Schröder, D.; Schwarz, H. *Angew. Chem., Int. Ed. Engl.* **1994**, *33*, 1174−1176.
(16) (a) Heinemann, C.; Wesendrup, R.; Schwarz, H. *Chem. Phys. Lett.* **1995**, *239*, 75−83. (b) Pavlov, M.; Blomberg, M. R. A.; Siegbahn, P. E. M.; Wesendrup, R.; Heinemann, C.; Schwarz, H. J. *Phys. Chem. A* **1997**, *101*, 1567−1579. (c) Achatz, U.; Beyer, M.; Joos, S.; Fox, B. S.; Niedner-Schatteburg, G.; Bondybey, V. E. J. *Phys. Chem. A* **1999**, *103*, 8200−8206. (d) Zhang, X. G.; Liyanage, R.; Armentrout, P. B. *J. Am. Chem. Soc.* **2001**, *123*, 5563−5575.
(17) Sievers, M. R.; Chen, Y. M.; Haynes, C. L.; Armentrout, P. M. *Int. J. Mass Spectrom.* **2000**, *195/196*, 149−170, and references therein.
(18) (a) van Koppen, P. A. M.; Kemper, P. R.; Bushnell, J. E.; Bowers, M. T. *J. Am. Chem. Soc.* **1995**, *117*, 2098−2099. (b) van Koppen, P. A. M.; Perry, J. K.; Kemper, P. R.; Bushnell, J. E.; Bowers, M. T. *Int. J. Mass Spectrom.* **1999**, *185/186/187*, 989−1001.
(19) (a) Zhang, Q.; Kemper, P. R.; Shin, S. K.; Bowers, M. T. *Int. J. Mass Spectrom.* **2001**, *204*, 281−294. (b) Haynes, C. L.; Armentrout, P. B.; Perry, J. K.; Goddard, W. A. *J. Phys. Chem.* **1995**, *99*, 6340−6346.
(20) (a) Musaev, D. G.; Morokuma, K. *J. Phys. Chem.* **1996**, *100*, 11600−11609. (b) Russo, N.; Sicilia, E. *J. Am. Chem. Soc.* **2001**, *123*, 2588−2596.
(21) Sicilia, E.; Russo, N. *J. Am. Chem. Soc.* **2002**, *124*, 1471−1480.
(22) (a) Rodriguez-Arias, E. N.; Rincon, L.; Ruette, F. *Organometallics* **1992**, *11*, 3677−3683. (b) Musaev, D. G.; Morokuma, K. *J. Chem. Phys.* **1994**, *101*, 10697−10707. (c) Hendrickx, M.; Gong, K.; Vanquickenborne, L. *J. Chem. Phys.* **1997**, *107*, 6299−6305. (d) Holthausen, M. C.; Fiedler, A.; Schwarz, H.; Koch, W. *Angew. Chem., Int. Ed. Engl.* **1995**, *34*, 2282−2285. (e) Holthausen, M. C.; Fiedler, A.; Schwarz, H.; Koch, W. *J. Phys. Chem.* **1996**, *100*, 6236−6242. (f) Holthausen, M. C.; Koch, W. *Helv. Chim. Acta* **1996**, *79*, 1939−1956.
(23) (a) Musaev, D. G.; Morokuma, K.; Koga, N.; Ngyen, K.; Gordon, M. S.; Cundari, T. R. *J. Phys. Chem.* **1993**, *97*, 11435−11444. (b) Hendrickx, M.; Ceulemans, M.; Vanquickenborne, L. *Chem. Phys. Lett.* **1996**, *257*, 8−14. (c) Perry, J. K.; Ohanessian, G.; Goddard, W. A. *J. Phys. Chem.* **1993**, *97*, 5238−5245.
(24) Yi, S. S.; Blomberg, M. R. A.; Siegbahn, P. E. M.; Weisshaar, J. C. *J. Phys. Chem. A* **1998**, *102*, 395−411.
(25) (a) Musaev, D. G.; Koga, N.; Morokuma, K. *J. Phys. Chem.* **1993**, *97*, 4064−4075. (b) Westerberg, J.; Blomberg, M. R. A. *J. Phys. Chem. A* **1998**, *102*, 7303−7307.
(26) Abashkin, Y. G.; Burt, S. K.; Russo, N. *J. Phys. Chem. A* **1997**, *101*, 8085−8093.
(27) Musaev, D. G.; Morokuma, K. *Isr. J. Chem.* **1993**, *33*, 307.
(28) Sändig, N.; Koch, W. *Organometallics* **1997**, *16*, 5244−5251.
(29) Perry, J. K.; Ohanessian, G.; Goddard, W. A. *Organometallics* **1994**, *13*, 1870−1877.
(30) Hada, M.; Nakatsuji, H.; Nakai, H.; Gyobu, S.; Miki, S. *J. Mol. Struct. (THEOCHEM)* **1993**, *281*, 207−212.
(31) (a) Plattner, D. A. *Angew. Chem., Int. Ed.* **1999**, *38*, 12−86. (b) Yarkony, D. R. *J. Phys. Chem.* **1996**, *100*, 18612−18628.
(32) (a) Shaik, S.; Danovich, D.; Fiedler, A.; Schröder, D.; Schwarz, H. *Helv. Chim. Acta* **1995**, *78*, 1393−1407. (b) Schröder, D.; Shaik, S.; Schwarz, H. *Acc. Chem. Res.* **2000**, *33*, 139−145.
(33) (a) Yarkony, D. R. *J. Phys. Chem. A* **1998**, *102*, 5305. (b) Manaa, M. R.; Chabalowski, C. F. *Chem. Phys. Lett.* **1999**, *300*, 619−625.
(34) Rue, C.; Armentrout, P. B.; Kretzschmar, I.; Schröder, D.; Harvey, J. N.; Schwarz, H. *J. Chem. Phys.* **1999**, *110*, 7858−7870.
(35) (a) Shaik, S.; Filatov, M.; Schröder, D.; Schwarz, H. *Chem. Eur. J.* **1998**, *4*, 193−199. (b) Harris, N.; Shaik, S.; Schröder, D.; Schwarz, H. *Helv. Chim. Acta* **1999**, *82*, 1784−1797. (c) de Visser, S. P.; Ogliaro, F.; Harris, N.; Shaik, S. *J. Am. Chem. Soc.* **2001**, *123*, 3037−3047.
(36) (a) Yoshizawa, K.; Shiota, Y.; Yamabe, T. *J. Chem. Phys.* **1999**, *111*, 538−545. (b) Yoshizawa, K.; Kagawa, Y. J. *Phys. Chem. A* **2000**, *104*, 9347−9355.
(37) (a) Stephens, P. J.; Devlin, F. J.; Chabalowski, C. F.; Frisch, M. J. *J. Phys. Chem.* **1994**, *98*, 11623−11627. (b) Becke, A. D. *Phys. Rev. A* **1998**, *38*, 3098−3100. (c) Becke, A. D. *J. Chem. Phys.* **1993**, *98*, 5648−5652. (d) Lee, C.; Yang, W.; Parr, R. G.. *Phys. Rev. B* **1988**, *37*, 785−789.

Scheme 1

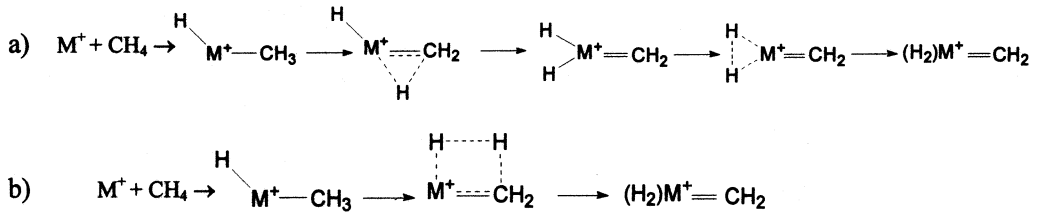

employed for replacing the chemically inert 60 core electrons ([Kr] $4d^{10}$ $4f^{14}$), and the 5s and 5p orbitals are treated explicitly along with the 5d, 6s, and 6p valence orbitals. The basis set for osmium is a modified LANL2DZ[39] double-ζ basis set plus an f-type polarization function,[40] (341/341/41/1), where the two outermost 6p functions of the standard LANL2DZ have been replaced by a (41) split of the optimized 6p function from Couty and Hall.[41] The standard triple-ζ 6-311G** basis set[42] of Pople and co-workers is used for carbon and hydrogen. Vibrational analyses are carried out for all stationary points for a 2-fold purpose. The first one is to check whether the optimized geometry corresponds to a minimum or a transition state. The second purpose is to obtain the zero-point vibrational energies (ZPVE) and Gibbs free energies. The total energies of all species are obtained by taking unscaled zero-point energy corrections into account. Intrinsic reaction coordinates (IRCs)[43] are traced from a transition state toward both reactant and product directions using the algorithm developed by Gonzalez and Schlegel[44] in the mass-weighted internal coordinate system. Each IRC is constructed from an accuracy of 0.1 $amu^{1/2}$·bohr. All calculations have been performed using the Gaussian 98 program.[45]

It is well known that the spin/orbital interaction is significant in the third-row transition metal or metal ion such as Os and Os^+. Since in our calculations spin/orbital effects are not accounted for, we need to know how the neglect of these effects will qualitatively influence the computed relative energies. First, we perform calculations on the ground state and first excited state of the osmium atom and the osmium ion and compare the calculated term splittings with the *J*-averaged excitation energies derived experimentally. We note that few experimental data are available for Os^+ except the energy levels of its ground term (^{6}D, $5d^66s^1$), but for Os the energy levels of both the ground term (^{5}D, $5d^66s^2$) and the lowest triplet term (^{3}F, $5d^76s^1$) were well assigned.[46] For example, in Os the *J*-averaged ^{5}D term is 2648.4 cm^{-1} (or 7.6 kcal/mol) above the experimental ground state $^5D_4$, and the *J*-averaged ^{3}F term is 1435.4 cm^{-1} (or 4.1 kcal/mol) higher in energy than the lowest $^3F_4$ level. The *J*-averaged splitting of the ^{3}F and ^{5}D terms is 28.0 kcal/mol for Os. This value is in good agreement with the calculated energy difference of 26.9 kcal/mol between the quintet ground state and the lowest triplet state. Besides this, the first ionization potential of Os is calculated to be 8.93 eV, being very close to the experimental value 8.7 eV.[47] Second, our calculations show that the bond dissociation energy $D([Os^+]-CH_2)$, a very important quantity for a description of the title reaction, is 112.4 kcal/mol. This value is comparable to the experimental value of ≥109.9 ± 1 kcal/mol[2b,12] and the value of 113 ± 3 kcal/mol suggested by Irikura and Goddard on the basis of MR-CISD calculations.[6a] Therefore, the B3LYP method with the selected basis set should be quite reliable in computing the relative energies of the species involved in the title reaction. On the other hand, although the spin/orbit stabilization is significant in Os^+, it may be quenched to a larger extent in Os^+-containing compounds because the electron distribution in a molecule is much more delocalized than in Os^+. Thus, we are confident that the neglect of spin/orbital effects does not change the qualitative features of the reaction mechanism captured by the present study.

3. Results and Discussions

The mechanism of the homologous kinds of reaction 1 was believed to involve the initial step which M^+ inserts into one C−H bond of CH_4 and yields initially a hydridomethyl complex, $HMCH_3^+$, followed by the activation of a second C−H bond and then the reductive elimination of H_2. In detail, two different possible mechanisms have been postulated (Scheme 1).

In pathway *a*, the activation of a second C−H bond proceeds through the methylene dihydride complex $HMH(CH_2)^+$, followed by the reductive elimination of H_2 to form a molecular hydrogen complex, $(H_2)MCH_2^+$, while in pathway *b*, the molecular hydrogen complex is directly obtained through a four-centered transition state. Previous investigations[11] have shown that those M^+ such as Ta^+ having enough valence electrons usually proceed through pathway *a*, whereas those M^+, such as Sc^+ and Ti^+, that do not have enough valence electrons often proceed through pathway *b*. The reaction of Os^+ with methane belongs to the former case, which will be confirmed in the present context.

Due to the possible spin crossovers involved in the reaction pathways, the potential energy profiles for the sextet, quartet, and doublet states are investigated. For the sake of simplicity, each species is labeled with its spin multiplicity as a superscript preceding the formula,

(38) (a) Hay, P. J.; Wadt, W. R. *J. Chem. Phys.* **1985**, 82, 270. (b) Wadt, W. R.; Hay, P. J. *J. Chem. Phys.* **1985**, 82, 284. (c) Hay, P. J.; Wadt, W. R. *J. Chem. Phys.* **1985**, *82*, 299.

(39) LANL2DZ: Dunning D95 basis sets on first row, Los Alamos ECP plus double-ζ basis sets on Na−Bi.

(40) Ehlers, A. W.; Böhme, M.; Dapprich, S.; Gobbi, A.; Höllwarth, A.; Jonas, V.; Köhler, K. F.; Stegmann, R.; Veldkamp, A.; Frenking, G. *Chem. Phys. Lett.* **1993**, *208*, 111−114.

(41) Couty, M.; Hall, M. B. *J. Comput. Chem.* **1996**, *17*, 1359−1370.

(42) Krishnan, R.; Binkley, J. S.; Seeger, R.; Pople, J. A. *J. Chem. Phys.* **1980**, *72*, 650.

(43) (a) Fukui, K. *J. Phys. Chem.* **1970**, *74*, 4161−4163. (b) Fukui, K. *Acc. Chem. Res.* **1981**, *14*, 363−368.

(44) Gonzalez, C.; Schlegel, H. B. *J. Phys. Chem.* **1990**, *94*, 5523−5527.

(45) Frisch, M. J.; Trucks, G. W.; Schlegel, H. B.; Scuseria, G. E.; Robb, M. A.; Cheeseman, J. R. Zakrzewski, V. G.; Montgomery, J. A., Jr.; Stratmann, R. E.; Burant, J. C.; Dapprich, S.; Millam, J. M.; Daniels, A. D.; Kudin, K. N.; Strain, M. C.; Farkas, O.; Tomasi, J.; Barone, V.; Cossi, M.; Cammi, R.; Mennucci, B.; Pomelli, C.; Adamo, C.; Clifford, S.; Ochterski, J.; Petersson, G. A.; Ayala, P. Y.; Cui, Q.; Morokuma, K.; Malick, D. K.; Rabuck, A. D.; Raghavachari, K.; Foresman, J. B.; Cioslowski, J.; Ortiz, J. V.; Baboul, A. G.; Stefanov, B. B.; Liu, G.; Liashenko, A.; Piskorz, P.; Komaromi, I.; Gomperts, R.; Martin, R. L.; Fox, D. J.; Keith, T.; Al-Laham, M. A.; Peng, C. Y.; Nanayakkara, A.; Challacombe, M.; Gill, P. M. W.; Johnson, B.; Chen, W.; Wong, M. W.; Andres, J. L.; Gonzalez, C.; Head-Gordon, M.; Replogle, E. S.; Pople, J. A. *GAUSSIAN 98* (release A.9); Gaussian, Inc.: Pittsburgh, PA, 1998.

(46) Moore, C. E. *Atomic Energy Levels*; Nat. Stand. Ref. Data Ser., Nat. Bur. Stand. (U.S.), 35 (reprint of NBS circular 467); U.S. Government Printing Office: Washington, DC, 1971; Vol. 3, pp 171−176.

(47) Weast, R. C., Lide, D. R., Astle, M. J., Beyer, W. H., Eds. *CRC Handbook of Chemistry and Physics*, 70th ed.; CRC Press Inc.: Boca Raton, New York; 1989−1990; pp E 80−81.

Table 1. Calculated Relative Energies ΔE_{Elec}(without ZPVE), ΔE_{Rel} (including ZPVE), and Relative Gibbs Free Energies ΔG_{298} (kcal/mol) of Stationary Points on the Potential Energy Surfaces of the Reaction $Os^+ + CH_4 \rightarrow OsCH_2^+ + H_2$ in the Sextet, Quartet, and Doublet States

	sextet			quartet			doublet		
species	ΔE_{elec}	ΔE_{rel}	ΔG_{298}	ΔE_{elec}	ΔE_{rel}	ΔG_{298}	ΔE_{elec}	ΔE_{rel}	ΔG_{298}
$Os^+ + CH_4$	0.0[a]	0.0[b]	0.0[c]	20.5	20.5	20.8	51.0	51.0	51.6
1	−13.1	−13.1	−9.0						
TS1/2	26.7	22.4	27.0						
2	−2.3	−5.7	−1.1	−38.5	−41.2	−36.4	−24.6	−27.4	−22.0
TS2/3	41.5	34.7	39.6	−9.6	−15.3	−10.0	−21.6	−25.1	−19.3
3	27.1	21.3	26.2	−18.4	−23.6	−18.3	−42.4	−46.7	−41.1
TS3/4	29.4	22.8	27.9	−8.8	−15.6	−10.6	−1.2	−5.8	0.1
4	19.3	13.4	18.0	−15.2	−20.1	−14.9	−1.7	−5.6	0.2
$5 + H_2$	31.7	22.9	30.5	3.5	−4.2	−5.5	10.3	2.5	1.7

[a] Absolute energy $E = -131.120886$ au. [b] Absolute energy $E = -131.076300$ au. [c] Absolute energy $E = -131.112703$ au.

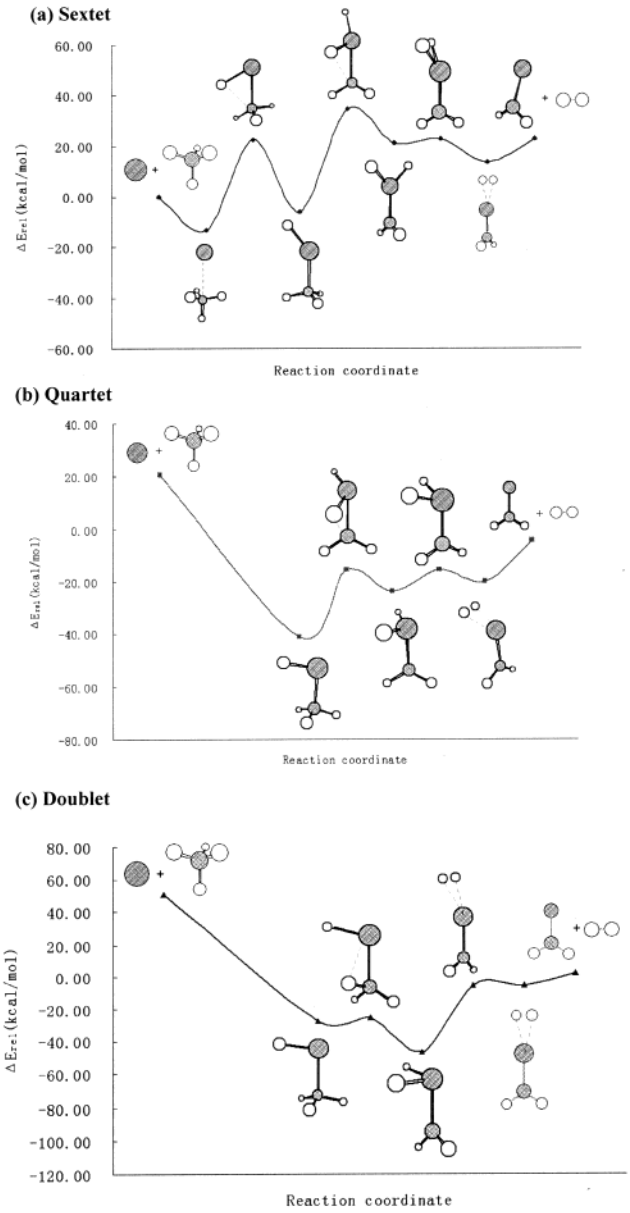

Figure 1. UB3LYP potential energy surfaces of the reaction $Os^+ + CH_4 \rightarrow OsCH_2^+ + H_2$ in the sextet (a), quartet (b), and doublet (c) states, respectively

while its spatial symmetry is omitted. The calculated potential energy profiles for the sextet, quartet, and doublet states are given in Figure 1, and the relative energies obtained for all stationary points on three potential energy profiles are collected in Table 1. The optimized geometries for all stationary points on three potential energy profiles are presented in Figure 2.

3.1. Sextet, Quartet, and Doublet Potential Energy Profiles. First, the sextet reaction path is shown in Figure 1a and Figure 2a. The reaction starts with the formation of the electrostatic η^3-methane complex $Os(CH_4)^+$ (^{6}**1**), which is 13.1 kcal/mol below the entrance channel $^6Os^+ + CH_4$. Then one C−H bond of methane oxidatively adds to the metal to form the hydridomethyl complex $HMCH_3^+$ (^{6}**2**), through the transition state ^{6}**TS1/2**. This step is endoergic by 7.4 kcal/mol, with a barrier of 35.5 kcal/mol. The third step is the activation of the second C−H bond of methane through the transition state ^{6}TS**2/3** to generate the methylene dihydride complex $HOsH(CH_2)^+$ (^{6}**3**), which is 27.0 kcal/mol higher in energy than ^{6}**2**. Next, the two hydrides bonded to the metal reductively eliminate to form the methylene dihydrogen complex $(H_2)Os(CH_2)^+$ (^{6}**4**), with an activation barrier of only 1.5 kcal/mol. Finally, ^{6}**4** would readily dissociate to produce the products $OsCH_2^+$ (^{6}**5**) and H_2. To summarize, one can see that the activation of the first C−H bond and of the second C−H bond, with barriers of 35.5 and 40.4 kcal/mol, respectively, are the rate-determining steps on the whole sextet reaction path. The whole reaction on this path is endothermic by 22.9 kcal/mol. For convenience in later discussions, hereafter we use H_1 and H_2 to denote the first and second hydrogens activated by Os^+, respectively.

Next let us turn to the quartet reaction path, as depicted in Figure 1b and Figure 2b. Different from that of the sextet path, the first step of the reaction on the quartet path is the formation of the hydridomethyl complex ^{4}**2**, which is a barrierless process. This result suggests that the oxidative addition of the first C−H bond by the excited state (^{4}F) of Os^+ is energetically spontaneous. We have undertaken a number of attempts to look for the corresponding encounter complex in the quartet state, but failed to find one. After ^{4}**2** is formed, one can see that the reaction processes on the quartet path are the same as those on the above-described sextet path. It should be pointed out that although numerous trials are taken to search for a possible four-membered cyclic transition state that connects ^{4}**2** and ^{4}**4** directly (Scheme 1b), no such transition state is obtained. Clearly, the activation of the second C−H bond through the transition state ^{4}**TS2/3** with a barrier of 25.9 kcal/mol is the slowest step on the quartet reaction path.

a) Sextet

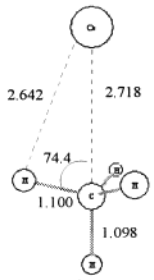

^{6}**1**

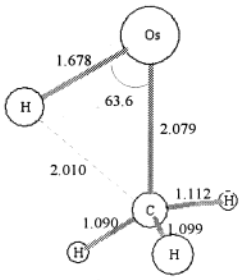

^{6}**TS1/2**

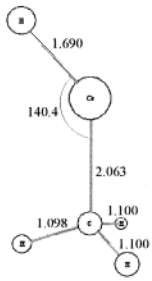

^{6}**2**

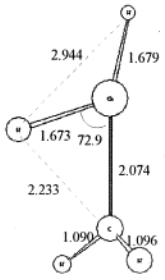

^{6}**TS2/3**

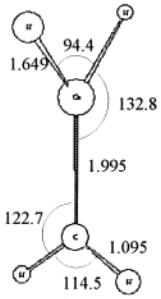

^{6}**3**

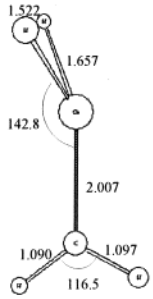

^{6}**TS3/4**

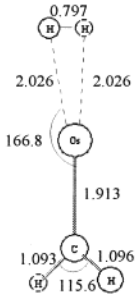

^{6}**4**

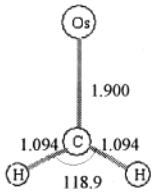

^{6}**5**

b) Quartet

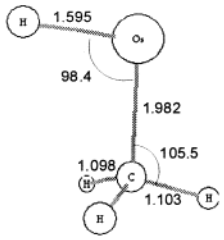

^{4}**2**

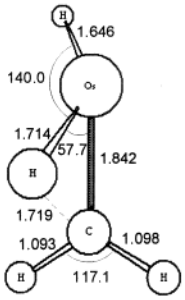

^{4}**TS2/3**

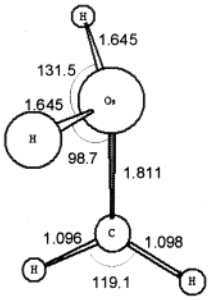

^{4}**3**

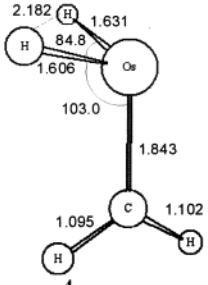

^{4}**TS3/4**

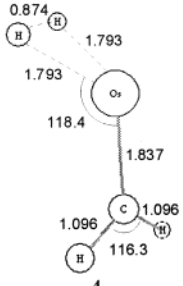

^{4}**4**

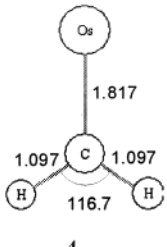

^{4}**5**

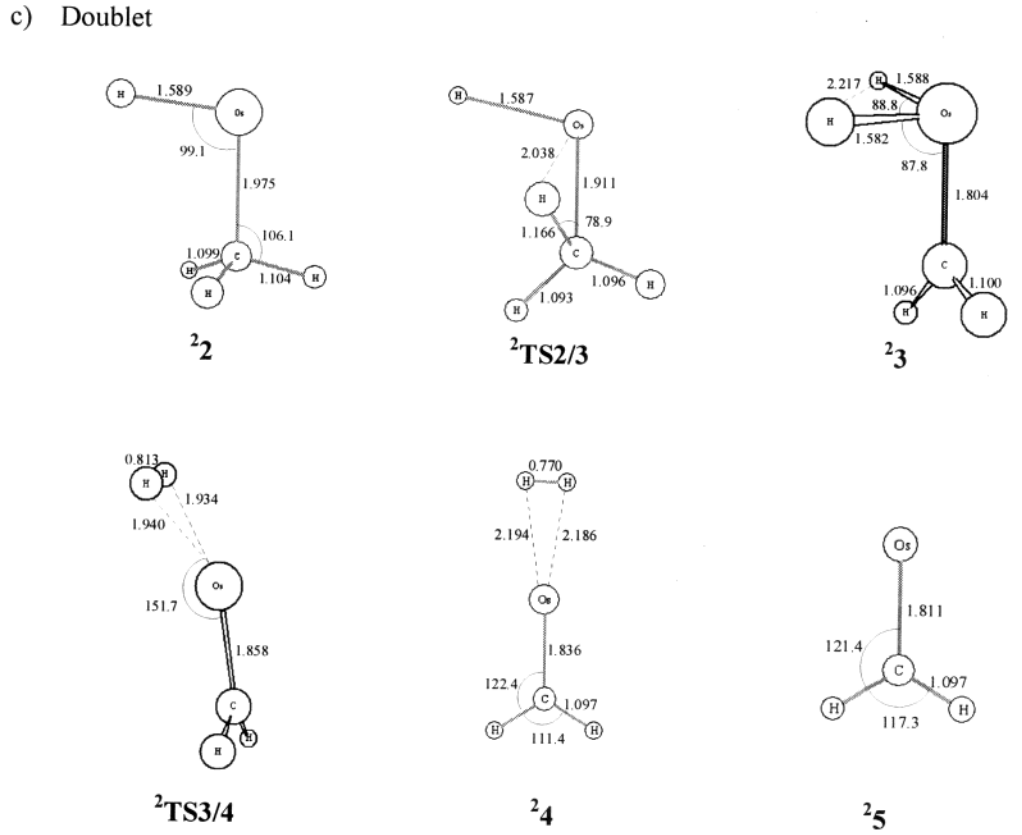

Figure 2. Optimized geometries for the stationary points of the reaction $Os^+ + CH_4 \rightarrow OsCH_2^+ + H_2$ in the sextet (a), quartet (b), and doublet (c) states (bond lengths in angstroms and bond angles in degrees).

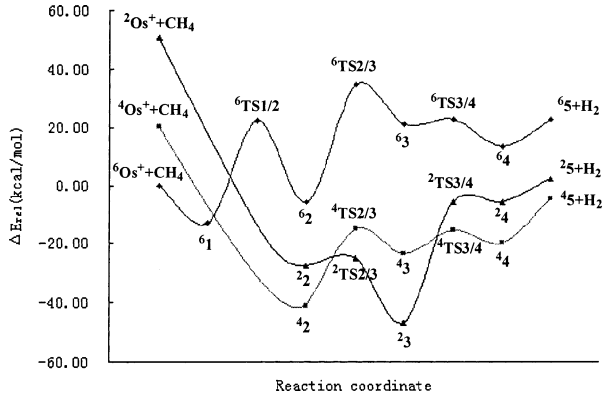

Figure 3. UB3LYP potential energy surfaces of the reaction $Os^+ + CH_4 \rightarrow OsCH_2^+ + H_2$ in the sextet, quartet, and doublet states.

As shown in Figure 1c and Figure 2c, methane dehydrogenation by Os^+ on the doublet path is very similar to that on the quartet one. The approach of methane to the excited state (^{2}H) of Os^+ also leads directly to the formation of the hydridomethyl complex ^{2}**2** without a barrier. Different from that on the quartet path, the oxidative addition of the second C−H bond to form the methylene dihydride complex ^{2}**3** is facile on the doublet path, with a barrier of only 2.3 kcal/mol. The rate-determining step on the doublet path is the reductive elimination of H_2 from ^{2}**3**, which requires 41.0 kcal/mol.

As seen from Figure 3, despite that the ground state of the reactants is $^6Os^+ + CH_4$, the most stable hydridomethyl complex is on the quartet surface (^{4}**2**), while among the methylene dihydride complexes, the doublet species ^{2}**3** has the lowest energy. For the methylene dihydrogen species and the final products, their relative order in stability is the same, i.e., ^{4}**4** > ^{2}**4** > ^{6}**4** and ^{4}**5** > ^{2}**5** > ^{6}**5**. Therefore, if methane dehydrogenation is readily activated by the ground-state Os^+, as observed experimentally, there must be crossings between the sextet and quartet, the quartet and doublet reaction surfaces, caused by the spin−orbital coupling. In the following, we will briefly discuss the geometries of all species occurring on three potential energy profiles and interpret the relative stabilities of those species with different multiplicities using the electron configurations of the metal ions and spin arguments.

3.2. Geometries and Stabilities of All Stationary Points on Three Potential Energy Profiles. The ground state of Os^+ is its sextet state ($5d^6 6s^1$), which lies 20.5 and 51.0 kcal/mol below the lowest quartet and lowest doublet states, respectively. The lowest quartet state of Os^+ has a $5d^7 6s^0$ electron configuration with two 5d orbitals doubly occupied, and the lowest doublet state also has a $5d^7 6s^0$ configuration but three 5d orbitals are doubly occupied. The difference in the electron configurations of the ground-state and excited-state Os^+ can be used to qualitatively understand the insertion reactivity of Os^+ into the C−H bond of methane. As is well known, oxidative addition of a C−H bond to a third-row metal center can be achieved by donation of the bonding σ electrons (of the C−H bond) into vacant 6s and $5d_\sigma$ orbitals of the metal and back-donation of metal $5d_\pi$ electrons into the antibonding σ^* orbital. According to this simple molecular orbital picture, metal states with empty 6s and $5d_\sigma$ orbitals tend to form a $HMCH_3^+$ intermediate directly. On the

other hand, metal states with an occupied 6s or $5d_\sigma$ orbital usually form a loosely bound complex MCH_4^+ because the replusive interactions between the 6s or $5d_\sigma$ electron and the bonding electrons of the C−H bond will compete with the electrostatic attraction between the metal cation and methane. In fact, this is the case we obtained for the reaction of Os^+ with methane. For the ground state of Os^+, our calculations lead to an encounter complex **^{6}1**, which is 13.1 kcal/mol below the entrance channel $^6Os^+ + CH_4$. This species has an η^3-H,H,H coordination mode, which is similar to those in the reaction systems of Rh^+ or Ta^+ with methane.[24,28] In contrast to the behavior of the ground-state Os^+, molecular orbital considerations would predict that the excited-state Os^+ (^{4}F,5d^{7}6s^0) and Os^+ (^{2}H,5d^{7}6s^0) react with methane to directly form the intermediate $HOsCH_3^+$ with corresponding multiplicity. This prediction is confirmed by our calculations. We have tried to find the corresponding intermediates on the quartet and doublet paths, but none of them are obtained.

The complex **^{6}TS1/2** is the transition state of the oxidative addition of the C−H_1 bond to the metal ion on the sextet path. In **^{6}TS1/2**, the activated C−H_1 bond is almost broken and the Os−H_1 bond is nearly formed, indicating that this transition state is a typical three-centered "late" transition state. **^{6}TS1/2** is 35.5 kcal/mol above the encounter complex **^{6}1** and 22.4 kcal/mol above the reactants $^6Os^+ + CH_4$.

For the hydridomethyl intermediate **2**, its ground state is a quartet state (i.e., **^{4}2**), which is 13.8 and 35.5 kcal/mol lower in energy than those of **^{2}2** and **^{6}2**, respectively. Geometrically, one can see that the Os−C and Os−H_1 bond distances are 2.063 and 1.690 Å in **^{6}2**, 1.982 and 1.595 Å in **^{4}2**, and 1.975 and 1.589 Å in **^{2}2**. These structural parameters show that the Os−C and Os−H_1 bonds are quite strong in **^{4}2** and **^{2}2**, but relatively weak in **^{6}2**. Natural bond orbital (NBO) analyses[48] suggest that in **^{4}2** and **^{2}2** two sd hybrid orbitals of Os^+ are bonded to the orbitals of the methyl and hydride ligands to form two covalent single bonds. The covalent Os−C and Os−H bonds formed in **^{4}2** and **^{2}2** are strong because the sd hybridization of osmium is effective due to the similarity in the size and energy of its 6s and 5d orbitals, which makes the overlap between the sd orbitals and the ligand orbitals fairly effective. As a consequence, the insertion of Os^+ into a C−H bond of methane is more exothermic than that of its first- and second-row homologues. In fact, this insertion process was calculated to be endothermic for Fe^+ [22a,b] and Ru^+.[5] Furthermore, NBO calculations show that the energy difference between **^{4}2** and **^{2}2** primarily can be understood in terms of the electronic configurations of the metal ion in both species. In both species, one 6s and one 5d orbital are involved in the formation of two covalent bonds; among the other four 5d orbitals one is doubly occupied and the other three 5d orbitals are all singly occupied. However, three unpaired electrons have the same spin in **^{4}2**, but one of them has to flip over in **^{2}2** to ensure doublet multiplicity. Thus the destabilization of **^{2}2** over **^{4}2** is mainly caused by the loss of some quantum mechanical exchange effects. For **^{6}2**, its weaker thermodynamic stability can be attributed to the weak Os−C bond because it is formed by a filled sd orbital and the sp^3 orbital of the carbon.

Similarly, the stabilities of the methylene dihydride species with different spin states can also be rationalized by their optimized geometries and NBO analyses. As displayed in Figure 2, the Os−C and Os−H bond lengths in **^{2}3** are 1.804 Å and ∼1.58 Å, respectively, both being shorter than those in **^{4}3** (1.811 and 1.645 Å) and in **^{6}3** (1.995 and 1.649 Å). The results listed in Table 1 show that **^{2}3** is 23.2 and 68.0 kcal/mol lower in energy than **^{4}3** and **^{6}3**. Clearly, the relative order of the stability of the methylene dihydride species, **^{2}3** > **^{4}3** > **^{6}3**, is reflected by the strength of the formed Os−C and Os−H bonds. Again, it is instructive to give a concise and qualitative description of the bonding mode in these species. In **^{2}3**, the metal uses one 6s orbital and three 5d orbitals to form two normal covalent bonds with two hydrides and a double bond with the methylene moiety. In addition, of the remaining two 5d orbitals, one is doubly occupied and the other one is singly occupied. Evidently, for the methylene dihydride Os(V) complex this bonding mode is optimal for the ion Os^+ only if the spin multiplicity of the species is a doublet. In contrast to the bonding mode in **^{2}3**, the double-bond character of the Os−C bond is reduced to some extent in **^{4}3**, and the Os−C bond becomes a single bond in **^{6}3**. Thus the weaker stability of **^{4}3** and **^{6}3** could be explained by the strength of the Os−C bond in these compounds.

The species **TS2/3** is the oxidative addition transition state of the C−H_2 bond to the metal ion. From the structures of each spin state, one can see that **^{6}TS2/3** and **^{4}TS2/3** are the three-centered "late" transition states, while **^{2}TS2/3** is a very "early" transition state. Energetically, **^{2}TS2/3** is 9.8 kcal/mol lower in energy than **^{4}TS2/3** and 59.8 kcal/mol below **^{6}TS2/3**. The relatively small barrier on the doublet path can be rationalized by the fact that the doublet state is not optimal for the hydridomethyl intermediate, but optimal for the methylene dihydride intermediate.

As for the methylene dihydrogen complex, we note that in **^{6}4** and **^{2}4** there exists only a relatively weak agostic interaction[49] between the dihydrogen ligand and the metal, as indicated by the calculated Os−(H_2) bond distances (about 2.03 Å in **^{6}4** and 2.19 Å in **^{2}4**). For **^{4}4**, the interaction between the dihydrogen ligand and the metal is stronger, which lengthens the H−H bond and shortens the Os−(H_2) bond. The structures of the methylene Os(III) products are very much like those of the Os═CH_2 part in the corresponding methylene dihydrogen species. The bonding modes in the methylene dihydrogen complexes, and the methylene Os(III) products with different multiplicities, are similar to those in the hydridomethyl intermediates with corresponding multiplicities, except that the orbital of the hydride ligand in the hydridomethyl intermediate is now replaced with the carbon $2P_\pi$ orbital of the methylene moiety. Thus, the quartet state is optimal for $OsCH_2^+$, in which a covalent double bond exists between Os and CH_2, as revealed from previous GVB calculations.[6a] More importantly, the relative stability order of the

(48) (a) Reed, A. E.; Weinstock, R. B.; Weinhold, F. *J. Chem. Phys.* **1985**, *83*, 735−746. (b) Reed, A. E.; Curtiss, L. A.; Weinhold, F. *Chem. Rev.* **1988**, *88*, 899−926.

(49) (a) Brookhart, M.; Green, M. L. H. *J. Organomet. Chem.* **1983**, *250*, 395−408. (b) Eisenstein, O.; Jean, Y. *J. Am. Chem. Soc.* **1985**, *107*, 1177−1186. (c) Calhorda, M. J.; Simões, J. A. M. *Organometallics* **1987**, *6*, 1188−1190.

methylene dihydrogen intermediates and the methylene Os(III) products should be the same as that of the hydridomethyl intermediates, as supported by the results shown in Figure 3.

It is also worthwhile to mention the structures of the reductive elimination transition state **TS3/4**. The transition states of the sextet and quartet states are about halfway between species **3** and **4**, but the doublet transition state is very "late". Since the quartet state is preferred for the methylene dihydrogen intermediate, but less favorable for the methylene dihydride intermediate, and the reverse is true for the species on the doublet path, one can easily understand that the barrier (7.9 kcal/mol) on the quartet path is considerably smaller than that (41.0 kcal/mol) on the doublet path.

3.3. Spin Crossing and the Possible Overall Reaction Path. In the above discussions, we can see that the minimum energy PES is not one of three PESs of a certain spin state. For example, for the sextet PES, the reactants $Os^+ + CH_4$ have the lowest energy, but the barrier of the first C−H activation (from ^{6}**2** to ^{6}**3**) is as high as 40.4 kcal/mol, and the overall reaction on the sextet path has an endothermicity of 22.9 kcal/mol. These results contradict the spontaneous dehydrogenation of methane by Os^+ observed experimentally. Thus, the crossing of adiabatic surfaces of different spin is involved in the processes of the title reaction. On the other hand, it is well known by now that transition-metal-mediated reactions very often occur on more than one adiabatic potential energy surface. Some experimental and theoretical evidence has been shown for the systems that include 3d, 4d, and some 5d transition metals.[20,21,25,26,28,29,35,36]

As shown in Figure 3, the minimum energy reaction path requires several possible spin crossings. First, the reaction may start with the formation of the encounter complex ^{6}**1** on the sextet PES. Then, the sextet surface should cross the quartet and doublet surfaces somewhere between ^{6}**1** and ^{6}**TS1/2**, since ^{6}**TS1/2** is too high in energy and the formation of the intermediate **2** on the doublet and quartet PESs is exothermic. After ^{4}**2** is formed, the reaction may jump to the doublet PES between **2** and **TS2/3** since ^{4}**TS2/3** is 9.8 kcal/mol above ^{2}**TS2/3** and the intermediate **3** on the doublet PES is thermodynamically much favored than the corresponding quartet species. Further, the reaction may jump back to the quartet PES in the reductive elimination step of dihydrogen (between **3** and **TS3/4**) since the barrier on the doublet path is as large as about 41.0 kcal/mol and the quartet product (^{4}**5**) is 6.8 kcal/mol more stable than the doublet product. To conclude, the minimum energy pathway may proceed as $^6Os^+ + CH_4 \rightarrow OsCH_4^+$ (^{6}**1**) $\rightarrow HOsCH_3$ (^{4}**2**) $\rightarrow$ ^{2}**TS2/3** $\rightarrow HOsH(CH_2)^+$ (^{2}**3**) $\rightarrow$ ^{4}**TS3/4** $\rightarrow (H_2)Os(CH_2)^+$ (^{4}**4**) $\rightarrow Os(CH_2)^+$ (^{4}**5**) $+ H_2$. If the reaction starts on the sextet PES and ends on the quartet PES, the overall reaction would occur thermodynamically at room temperature, and it would be exothermic by 4.2 kcal/mol, as listed in Table 1. But if the reaction ends up with the doublet product, the total reaction would be endothermic by 2.5 kcal/mol. Thus, our results support that the reaction ends on the quartet PES. However, in either case the calculated results can reasonably explain the experimental observations. Further state-specific reactivity measurements are required to compare with our results here.

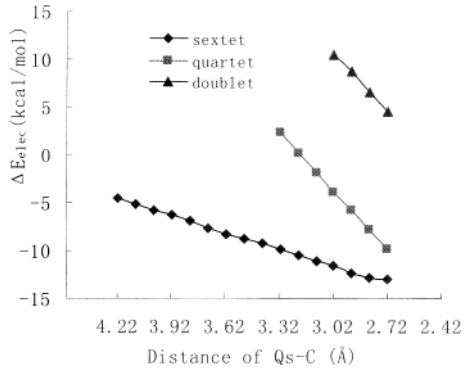

Figure 4. Sextet, quartet, and doublet potential energies of the reactant complex as a function of the distance between Os^+ and the carbon atom of CH_4.

3.4. Crossing Points between the PESs of Different Multiplicities. To better understand the spin inversion processes described above, it is instructive to locate the crossing points between the sextet and quartet PESs, and between the quartet and doublet PESs, on the reaction pathway. Since the potential energy of the reaction system ($Os^+ + CH_4$) has 12 internal degrees of freedom, it is prohibitive to give full descriptions of the crossing seam between the two PESs, which is a "line" of dimension 11. Although several efficient algorithms[50−53] have been developed for the location of surface crossings, the implementation of these algorithms within the context of DFT is not available in the Gaussian 98 program. Thus we choose a simple approach suggested by Yoshizawa et al.[36] for approximately locating the crossing points of two PESs of different multiplicities. The main idea of this approach is to perform a series of single-point computations of one spin state along the IRC of the other spin state and vice versa. It should be mentioned that the crossing points obtained in this way are approximations to true minimum energy crossing points (MECPs) as determined from other approaches,[50−53] but the energies of these crossing points provide upper bounds to those of the corresponding MECPs.

At first, computed potential energy profiles of the sextet, quartet, and doublet states, respectively, as a function of the distance between Os^+ and CH_4, are depicted in Figure 4. For a given Os−C bond length, all other geometrical degrees of freedom are optimized for each spin state. As shown in Figure 4, as methane approaches the metal, the energy of the complex descends monotonically for each spin state. Since the energies of the complex in the quartet and doublet states are always above that in the sextet state, no crossing points between the sextet and quartet (or doublet) PESs occur before the formation of the sextet reactant complex ^{6}**1**.

(50) Koga, N.; Morokuma, K. *Chem. Phys. Lett.* **1985**, *119*, 371−374.
(51) Yarkony, D. R. *J. Phys. Chem.* **1993**, *97*, 4407−4412.
(52) Bearpark, M. J.; Robb, M. A.; Schlegel, H. B. *Chem. Phys. Lett.* **1994**, *223*, 269−274.
(53) Harvey, J. N.; Aschi, M.; Schwarz, H.; Koch, W. *Theor. Chem. Acc.* **1998**, *99*, 95−99.

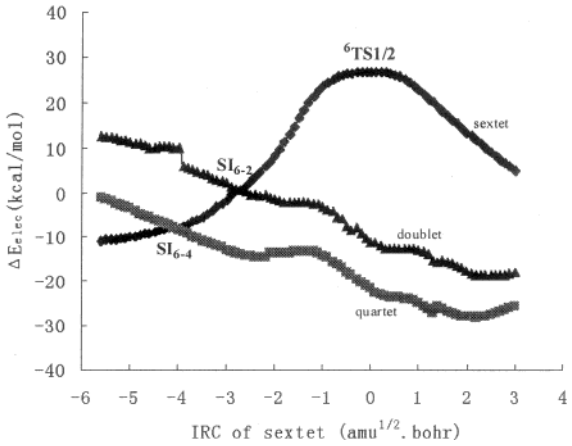

Figure 5. Potential energies from the reactant complex to the hydridomethyl complex **2** along the sextet IRC.

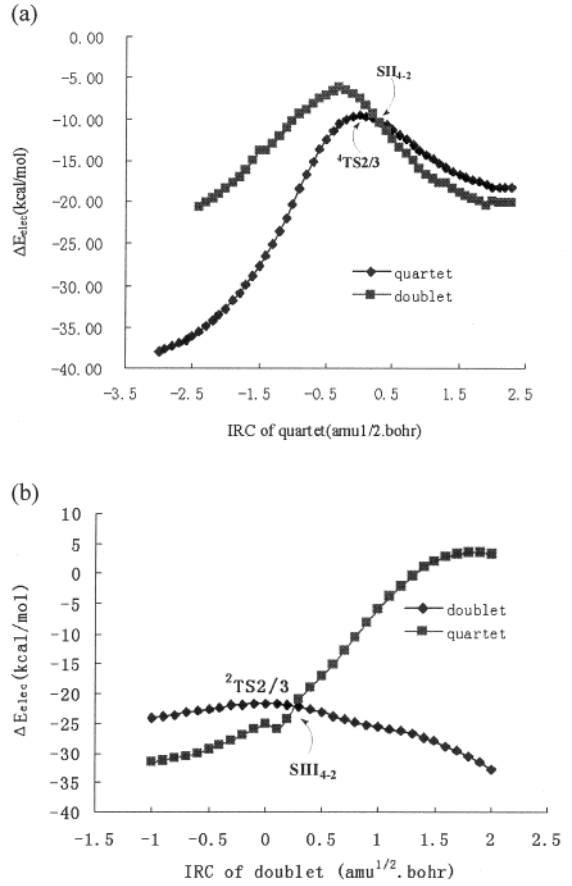

Figure 6. Potential energies from the hydridomethyl complex **2** to the methylene dihydrido complex **3** along (a) the quartet IRC and (b) the doublet IRC.

Let us turn to the crossing points between the sextet and quartet (or doublet) surfaces in the region from the encounter complex **1** to the hydridomethyl complex **2**.

Figure 5 shows computed potential energy profiles of the doublet, quartet, and sextet states along the sextet IRC. The IRC is traced from ^{6}**TS1/2** (IRC = 0) toward both reactant (IRC < 0) and product (IRC > 0) directions. Two crossing points, **SI**$_{6-4}$ between the sextet and quartet PESs and **SI**$_{6-2}$ between the sextet and doublet surfaces, are located before ^{6}**TS1/2**. **SI**$_{6-4}$ is situated at IRC = −4.05 with a relative energy of 5.1 kcal/mol with respect to ^{6}**1**, and **SI**$_{6-2}$ lies at IRC = −2.75 with a relative energy of 13.6 kcal/mol with respect to ^{6}**1**. The

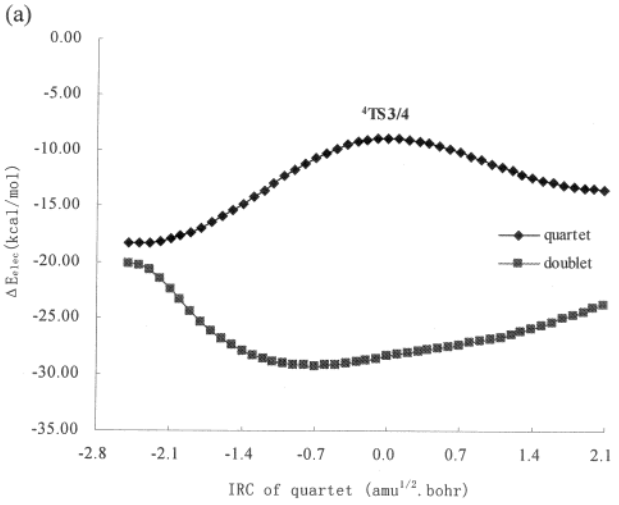

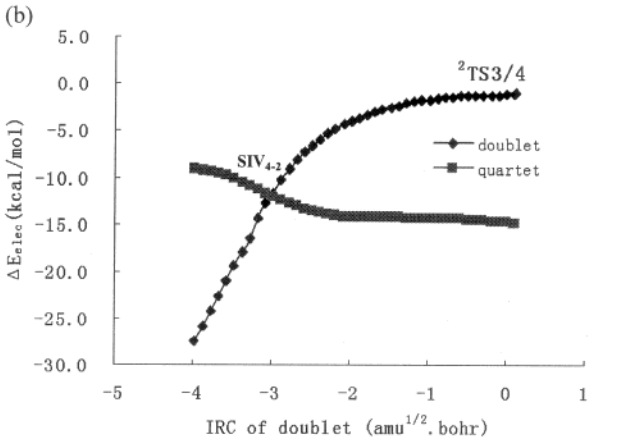

Figure 7. Potential energies from the methylene dihydrido complex **3** to the product dihydrogen complex **4** along (a) the quartet IRC and (b) the doublet IRC.

structures of **SI**$_{6-4}$ and **SI**$_{6-2}$ are shown in Figure 8. As seen from Figure 5, after passing point **SI**$_{6-4}$, the quartet PES can provide a low-energy reaction pathway toward the hydridomethyl complex **2**. In fact, as shown in Figure 3, the formation of **2** on the quartet or doublet surfaces is a barrierless process. Therefore, the reacting system is most likely to change its spin multiplicity from the sextet state to the quartet state in the oxidative addition step of the first C−H bond.

Similarly, we show computed potential energy profiles of the doublet and quartet states along the quartet IRC (from **2** to **3**) in Figure 6a and along the doublet IRC in Figure 6b. In Figure 6a, one can see that a crossing point **SII**$_{4-2}$ is located at IRC = 0.30 with an energy of 28.1 kcal/mol relative to that of ^{4}**2**. In Figure 6b, another crossing point **SIII**$_{4-2}$ is found at IRC = 0.25, the energy being 16.6 kcal/mol higher than ^{4}**2**. The structures of both crossing points are given in Figure 8. According to Yoshizawa et al.,[36a] **SIII**$_{4-2}$ is the energy-minimum crossing point, and **SII**$_{4-2}$ is the energy-maximum crossing point between the quartet and doublet surfaces in the reaction pathway from **2** to **3**. Therefore, there is a crossing seam between **SII**$_{4-2}$ and **SIII**$_{4-2}$. The reacting system should change its spin multiplicity from the quartet state to the doublet state in this crossing region and then move on the doublet potential energy surface as the reaction goes on.

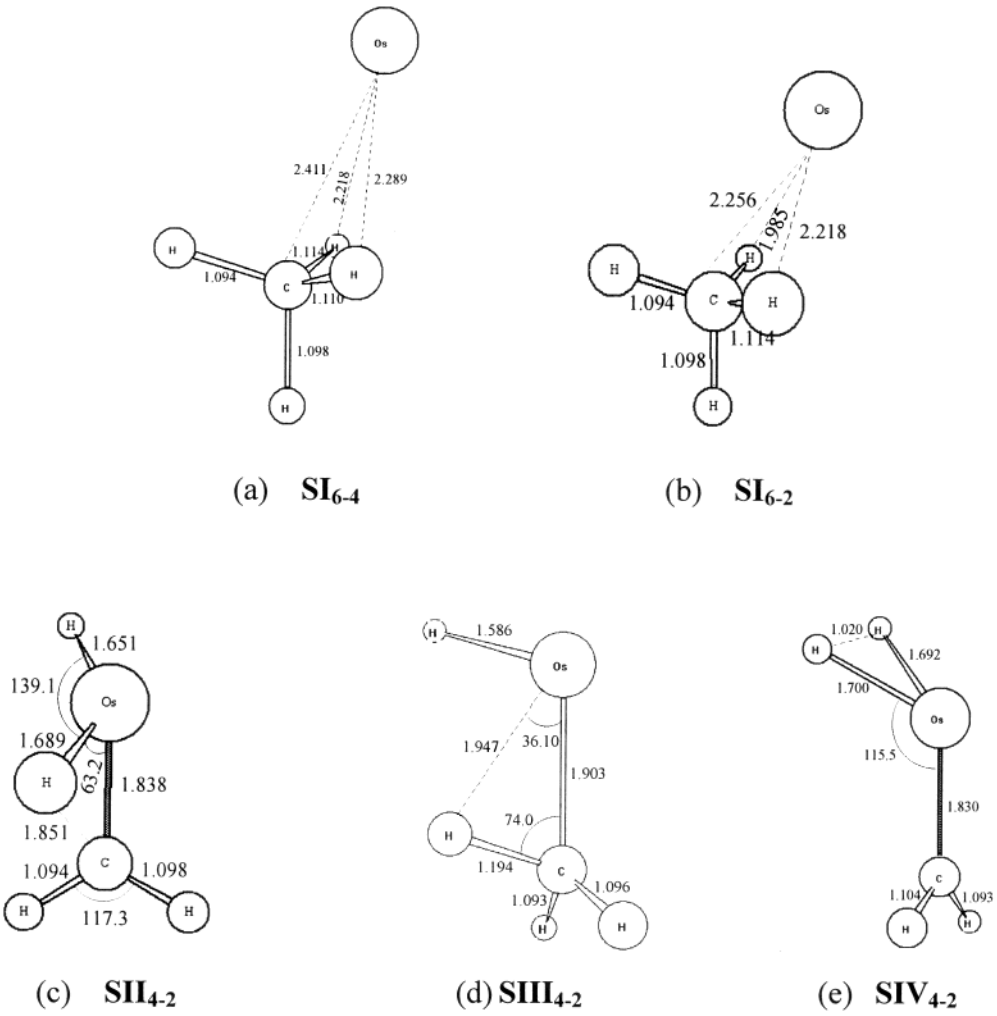

Figure 8. Structures of the crossing points: (a) between sextet and quartet; (b) between sextet and doublet; (c) the energy-maximum point between quartet and doublet before **TS2/3**; (d) the energy-minimum point between quartet and doublet before **TS2/3**; (e) between quartet and doublet before **TS3/4**.

Figure 7 gives the potential energy profiles of the doublet and quartet states from the methylene dihydrido intermediate **3** to the methylene dihydrogen complex **4** along the quartet and doublet IRCs, respectively. Along the quartet IRC no crossing point is found, but along the doublet IRC we find a crossing point, $\mathbf{SIV}_{4-2}$, which is at IRC = −3.02 (before ^{2}**TS3/4**) with a relative energy of 30.4 kcal/mol above ^{2}**3**. The structure of this crossing point is also collected in Figure 8. From the distance between the two hydrides (1.020 Å) in $\mathbf{SIV}_{4-2}$, one can see that $\mathbf{SIV}_{4-2}$ is closer to the methylene dihydorgen complex ^{4}**4** than the transition state ^{4}**TS3/4**. Energetically, $\mathbf{SIV}_{4-2}$ is only 3.8 kcal/mol above ^{4}**4**. Thus, the reaction may jump from the doublet PES to the quartet PES near the crossing point $\mathbf{SIV}_{4-2}$ without passing the transition state ^{2}**TS3/4**. As a consequence, the barrier of the reductive elimination of H_2 from ^{2}**3** to ^{4}**4** would decrease from 41.0 to 30.4 kcal/mol. Although this step is still thermodynamically unfavorable, it may happen because it is coupled to other reaction steps that are strongly exothermic, such as the oxidative addition of the first C−H bond (from ^{6}**1** to ^{4}**2**).

4. Conclusions

Density functional calculations have been performed to investigate the mechanism of methane dehydrogenation by gas-phase Os^+. The sextet, quartet, and doublet potential energy surfaces of the title reaction have been explored. The following conclusions can be draw from the present calculations.

a. The minimum energy reaction path is found not to be one of three PESs of a certain spin state. Instead, the minimum energy reaction path requires the crossing of two adiabatic surfaces with different spin states in the different reaction steps. Totally, three spin states are involved in the whole reaction. This result is different from that in methane dehydrogenation by other transition-metal ions such as Fe^+, in which two spin states are usually involved. Specifically, the minimum energy pathway can be described as $^6Os^+ + CH_4 \rightarrow OsCH_4^+$ (^{6}**1**) → $HOsCH_3$ (^{4}**2**) → $HOsH(CH_2)^+$ (^{2}**3**) → $(H_2)Os(CH_2)^+$ (^{4}**4**) → $Os(CH_2)^+$ (^{4}**5**) + H_2.

b. The reacting system should change its spin multiplicity three times in the whole reaction processes. The first spin inversion, from the sextet state to the quartet state, occurs near the crossing point $\mathbf{SI}_{6-4}$. After passing this point, the reacting system moves on the quartet PES toward the hydridomethyl complex **2**. The second crossing seam exists between $\mathbf{SII}_{4-2}$ and $\mathbf{SIII}_{4-2}$, in the region where the second C−H bond of methane is being activated. An important consequence of this spin conversion from the quartet state to the doublet state is

that the barrier of the second C−H bond cleavage decreases from 25.9 to 16.1 kcal/mol. The third spin inversion occurs from the doublet state to the quartet state near the crossing point **SIV**$_{4-2}$, and then the reaction would prefer to proceed on the quartet potential energy surface until the end of the reaction. This spin inversion leads to a decrease in the reductive elimination barrier height from 41.0 to 30.4 kcal/mol. Therefore, the rate-limiting step in the whole reaction is the reductive elimination of dihydrogen from the doublet methylene dihydride species, with a barrier of about 30.4 kcal/mol.

c. If the reaction starts on the sextet PES and ends on the quartet PES, the overall reaction is calculated to be exothermic by 4.2 kcal/mol, which is in good agreement with the available experimental results.

Acknowledgment. This work was supported by the National Natural Science Foundation of China (Grant No. 20073020). We are grateful to the referees for their pertinent comments and good suggestions concerning our original manuscript. Partial computations are carried out on the SGI Origin 3800 and Dawning 3000A at Nanjing University.

OM030291V